www.nature.com/modpathol

ARTICLE

Genomic landscape of endometrial carcinomas of no specific molecular profile

Amir Momeni-Boroujeni[1], Bastien Nguyen[2,3], Chad M. Vanderbilt[1], Marc Ladanyi[1], Nadeem R. Abu-Rustum[4], Carol Aghajanian[5], Lora H. Ellenson[1], Britta Weigelt[1,6]✉ and Robert A. Soslow[1,6]✉

Endometrial carcinomas (ECs) classified by The Cancer Genome Atlas (TCGA) as copy number-low (also referred to as "no specific molecular profile" [NSMP]) have a prognosis intermediate between *POLE*-mutated and copy number-high ECs. NSMP-ECs are a heterogeneous group, however, comprising both relatively indolent and aggressive ECs. We identified a total of 472 NSMP-ECs among 1,239 ECs that underwent clinical sequencing of 410–468 cancer-related genes. Somatic mutation and copy number alteration data were subjected to unsupervised hierarchical clustering, which identified three genomic clusters. Random sampling with stratification was used to choose ~80 endometrioid ECs from each cluster, resulting in a study size of 240 endometrioid ECs as well as an additional 44 non-endometrioid NSMP-ECs. Cluster 1 (C1, $n = 80$) consisted primarily of NSMP-ECs with *PTEN* and *PIK3R1* mutations, Cluster 2 (C2, $n = 81$) of tumors with *PTEN* and *PIK3CA* mutations and Cluster 3 (C3, $n = 79$) of NSMP-ECs with chromosome 1q high-level gain and lack of *PTEN* mutations. The majority (72.7%) of non-endometrioid NSMP-ECs mapped to C3. NSMP-ECs from C3 were more likely to be FIGO grade 3 (30%), estrogen receptor-negative/weak (54.5%) and FIGO stages III or IV. In multivariate analysis, molecular clusters were associated with worse overall survival outcomes with C3 tumors having the worst (hazard ratio: 4) and C1 tumors having the best outcome. In conclusion, NSMP-ECs are a heterogenous group of tumors and comprise both aggressive and clinically low-risk ECs that can be identified based on mutation and copy number data.

Modern Pathology (2022) 35:1269–1278; https://doi.org/10.1038/s41379-022-01066-y

INTRODUCTION

Molecular profiling of endometrioid and serous carcinomas of the endometrium by The Cancer Genome Atlas (TCGA) revealed four genomic groups, which include ultramutated tumors with *POLE* exonuclease domain mutations, hypermutated tumors with microsatellite instability (MSI)/ DNA mismatch repair (MMR) deficiency, copy number-high tumors with *TP53* mutations, and copy number-low tumors, which lack all of the above-mentioned alterations[1]. The latter group was shown to be composed of tumors with predominately endometrioid morphology and considerable molecular heterogeneity, which has since been referred to as endometrial carcinoma (EC) of no specific molecular profile (NSMP)[2]. Follow-up studies suggested an exclusion surrogate approach (ProMisE) for identifying NSMP-EC, whereby ECs harboring any characteristic of the other TCGA groups are excluded, i.e. tumors lacking *POLE* exonuclease domain mutations, are MMR-proficient, and are p53/*TP53* wild-type are designated as NSMP-ECs[3,4]. The designation of NSMP to this group of ECs derives from considerable molecular heterogeneity of this group and absence of defining molecular features. Additionally, the NSMP-EC have been shown to be a clinically and histologically diverse.

The molecular heterogeneity of NSMP-ECs has been shown to have clinical relevance[5]. For example, it has been reported that NSMP-ECs harboring 1q32.1 high level gain[6,7], *CTNNB1* hotspot mutations[7] or expression of L1CAM[8] are associated with adverse outcomes.

Given the heterogeneity observed in NSMP-EC, one of the largest molecular subgroups of EC, in-depth studies are needed to further refine and understand the molecular underpinnings of these tumors[9]. In this study, we sought to define the clinicopathologic and molecular characteristics of a large group of NSMP-ECs subjected to clinical sequencing of 410–468 cancer-related genes and attempt to subclassify these tumors based on characteristic molecular findings.

MATERIALS AND METHODS

Case selection and data extraction

This study, including review and analysis of data, was approved by the Institutional Review Board at Memorial Sloan Kettering Cancer Center (MSK). ECs of all histologic types that underwent clinical tumor-normal targeted DNA next-generation sequencing (NGS) of 410–468 cancer-related genes using MSK-Integrated Mutation Profiling of Actionable Cancer Targets (MSK-IMPACT)[10,11] between 2014 and 2019 were evaluated ($n = 1,239$). ECs of the NSMP-EC molecular subtype class in this MSK-IMPACT cohort were identified by employing a surrogate of the ProMisE model[12], as previously described[13]: tumors with hotspot *POLE* exonuclease

[1]Department of Pathology and Laboratory Medicine, Memorial Sloan Kettering Cancer Center, New York, NY, USA. [2]Marie-Josée and Henry R. Kravis Center for Molecular Oncology, Memorial Sloan Kettering Cancer Center, New York, NY, USA. [3]Human Oncology and Pathogenesis Program, Memorial Sloan Kettering Cancer Center, New York, NY, USA. [4]Gynecology Service, Department of Surgery, Memorial Sloan Kettering Cancer Center, New York, NY, USA. [5]Department of Medicine, Memorial Sloan Kettering Cancer Center, New York, NY, USA. [6]These authors jointly supervised this work: Britta Weigelt, Robert A. Soslow. ✉email: weigeltb@mskcc.org; soslowr@mskcc.org

Received: 19 October 2021 Revised: 22 February 2022 Accepted: 23 February 2022
Published online: 1 April 2022

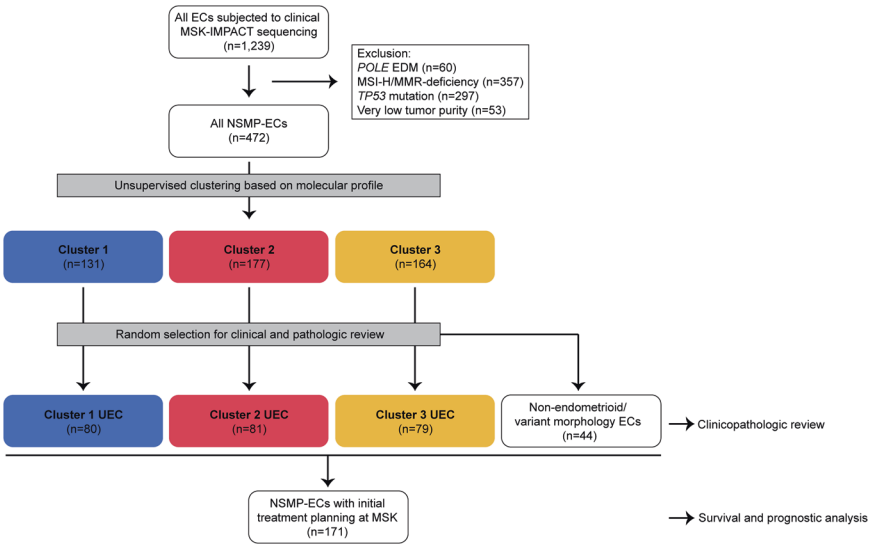

Fig. 1 CONSORT diagram summarizing the selection process of NSMP endometrial carcinomas included in this study. NSMP-EC, endometrial carcinomas of no special molecular profile; EDM, exonuclease domain mutant; MMR, DNA mismatch repair; MSI, microsatellite instability.

domain mutations ($n = 60$), with DNA MMR-deficiency defined either by immunohistochemistry and/or genomic determination (high MSIsensor score; $n = 357$)[14], and with aberrant p53 immunohistochemical expression or *TP53* genetic alterations including somatic mutations and homozygous deletions ($n = 297$) were excluded. In addition, to ensure high quality data, sequenced tumors with very low tumor purity (<10% as estimated by the reviewing pathologist or average variant allele frequency <5%) were excluded from the analysis ($n = 53$). The remaining cases were included in the downstream analysis ($n = 472$; see CONSORT diagram Fig. 1).

Genomic data

The MSK-IMPACT assay assesses somatic mutations, copy number (CN) alterations, structural variants, fraction of genome altered (FGA) and tumor mutation burden (TMB), as previously described[13]. GISTIC (version 2.0.23) was used to analyze the broad CN data[15]. The mutational data included chromosomal location, base-pair change, protein change, predicted functional impact of the mutation and the associated variant frequency. Data on allele specific CN alterations and ploidy were extracted using the 'facets' R package (version 0.5.14)[16]. Cancer cell fractions (i.e. clonality) of all somatic mutations were inferred using ABSOLUTE (v1.0.6), as described previously[17] using CN and tumor purity estimation information derived from FACETS[16]. Mutational signatures were determined using the MuSiCa R application (version 1.0)[18] in samples harboring ≥5 mutations (both synonymous and non-synonymous). Annotation of the genomic alterations for oncogenic properties was performed using the OncoKB database, as previously described[19]. Evaluation for mutual exclusivity/co-occurrence was performed using the 'DISCOVER' R package (v0.9)[20].

Pathology review

The histopathologic and morphologic data were extracted from the synoptic pathology report. The scanned pathology slides of the sequenced tumor were reviewed by a gynecologic pathologist (A.M.-B.) to confirm the findings of the pathology report. For histologic typing, to mitigate the effect of suboptimal interobserver concordance[21,22], we performed a single-institution study with a group of experienced gynecologic pathologists. Biweekly diagnostic consensus conferences encouraged a uniform diagnostic approach within the group, as did frequent review of each other's cases for tumor board and quality assurance, as described[13].

Clustering and statistical analysis

A reduced segments matrix was calculated from the FACETS-derived CN segmentation file using the CNTools R package. The CN and the cancer cell fraction of somatic mutations were then used to create a combined data matrix which was subsequently normalized. Principal component (PC) analysis (PCA) was used to reduce the dimensionality of the matrix by employing the fast.prcomp function of the gmodels R package. Thirteen statistically significant PCs were identified using a permutation test. The output was visualized using t-distributed stochastic neighbor embedding (T-SNE; 'rtsne' R package; Supplementary Fig. S1)[23]. To identify tumor clusters in our dataset, partitioning into separate clusters based on their scores along the thirteen significant PCs was performed using the HDBSCAN function of the DBSCAN R package[24].

Comparisons of quantitative data between the groups were performed using ANOVA with post-hoc Tukey test and comparison of qualitative data including associations between clinicopathologic features and molecular data were performed using chi-squared test with Fisher's exact p value calculation. All p value were two tailed and p values <0.05 were considered statistically significant. Disease-free survival (DFS) and overall survival (OS) were evaluated by calculating survival curves using the Kaplan–Meier method, using the Log-rank test to compare subgroups, with the start date set as the date of initial diagnostic biopsy. Univariate and multivariate Cox Proportional Hazards analysis was performed to determine the hazard ratio (HR).

Final case selection

Following genomic clustering, an equal number of endometrioid ECs were selected from each genomic cluster for further downstream analysis using random sampling with stratification ($n = \sim 80$ sample for each of three clusters; Fig. 1). In addition, 44 non-endometrioid ECs or endometrioid variants meeting the same criteria used for NSMP-EC were selected and analyzed separately; these tumors consisted of 15 high-grade ECs with ambiguous morphology, nine endometrial clear cell carcinomas, seven mesonephric-like carcinomas, five carcinosarcomas, two corded and hyalinized endometrioid carcinomas, two dedifferentiated ECs, two undifferentiated ECs and two uterine serous carcinomas. The pathology reports and histopathology slides were reviewed for the 240 uterine endometrioid carcinomas and the 44 non-endometrioid/ variant endometrioid ECs, and clinical data relating to disease presentation and course were extracted from the electronic health records (Fig. 1).

RESULTS

A large series of 472 NSMP-ECs subjected to clinical FDA-authorized tumor-normal MSK-IMPACT sequencing of 410–468 cancer-related genes, which included primarily uterine endometrioid carcinomas (UECs; $n = 367$), but also non-endometrioid ECs and/or tumors with variant endometrioid histology ($n = 105$), were clustered based on mutational and gene CN alteration data. Specifically, in this initial cohort of NSMP-EC ($n = 472$), UEC was the most common tumor histologic type (367/472, 77.8%), followed by high-grade ECs with ambiguous morphology (46/472, 9.7%), uterine clear cell carcinoma (23/472, 4.9%), mesonephric-like carcinoma (12/472, 2.5%), uterine carcinosarcoma (9/472, 1.9%) with rare tumors categorized as uterine serous carcinoma (6/472, 1.3%), corded and hyalinized

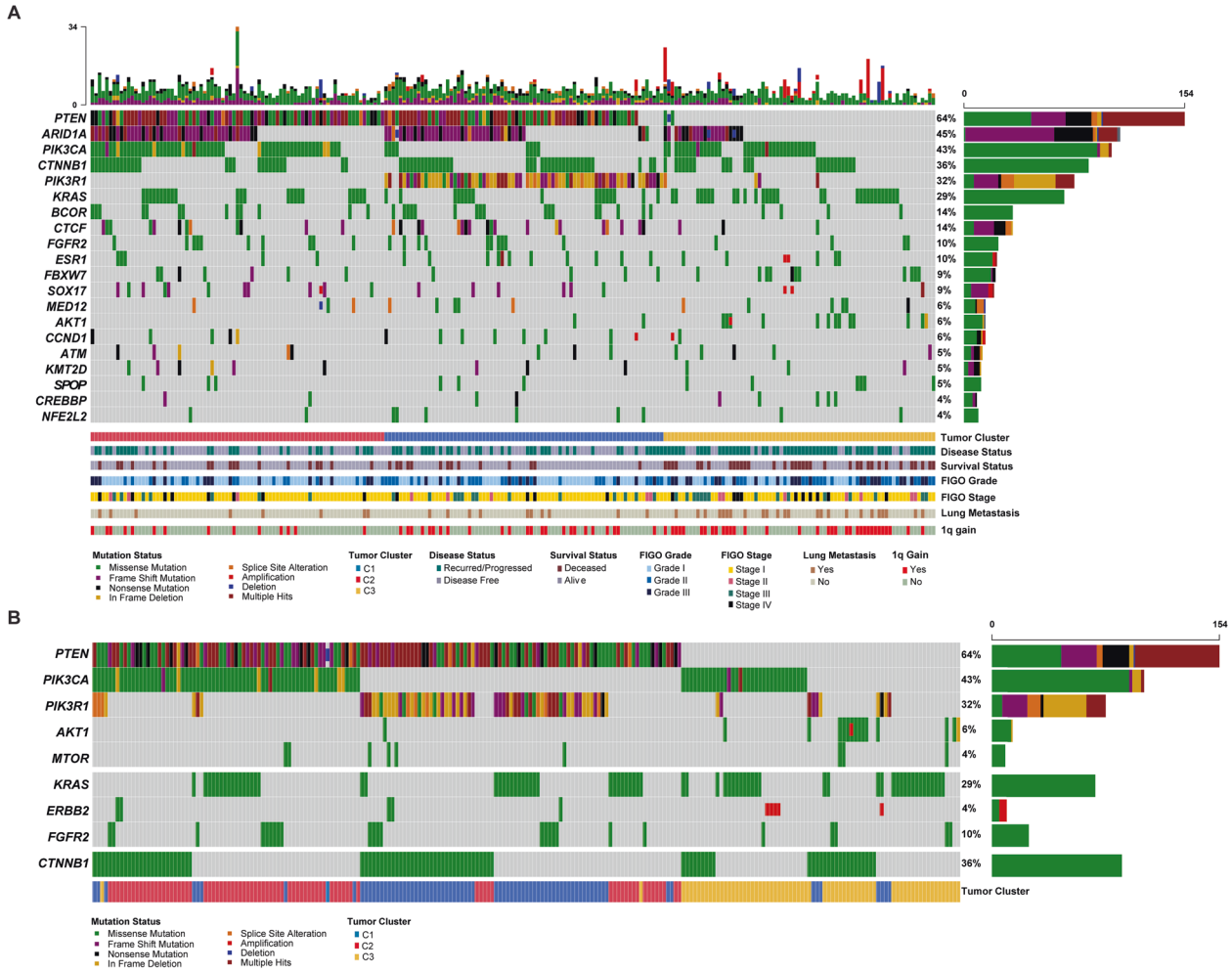

Fig. 2 Recurrent somatic genetic alterations in NSMP uterine endometrioid carcinomas. A Oncoprint depicting the most recurrent genomic alterations in uterine endometrioid carcinomas of no special molecular profile (NSMP-UEC). Each column represents a tumor with the bar graph at the top depicting the number/distribution of alterations per sample, and the Oncoprint rows showing alterations for each gene. The bottom part of the graph shows the summary of histopathologic and clinical information for each case. The bar graph on the right of the panel shows the number and distribution of alterations for each gene. Mutation types and clinicopathologic features are color-coded according to the legend. **B** Oncoprint depicting the most recurrent molecular alterations in NSMP-UEC focusing on alterations activating the PI3K/AKT/mTOR pathway in addition to *CTNNB1* alterations. The bottom part of the graph shows the summary of molecular cluster information for each case. Note that majority of tumors harbor a combination of *PIK3CA*/*PIK3R1* and *PTEN* mutations while *AKT1* mutations occur in absence of upstream alterations. *KRAS*, *ERBB2* and *FGFR2* alterations are mutually exclusive. Mutation types and other features are color-coded according to the legend. C1, Cluster 1; C2, Cluster 2; C3, Cluster 3.

endometrioid carcinoma (4/472, 0.8%), dedifferentiated carcinoma (3/472, 0.6%), and undifferentiated carcinoma (2/472, 0.4%). The majority of UECs were FIGO grade 1 tumors (199/367, 54.2%), followed by FIGO grade 2 (97/367, 26.4%) and FIGO grade 3 (71/367, 19.3%) tumors.

The clustering revealed the presence of 3 distinct clusters: cluster 1 (C1), cluster 2 (C2) and cluster 3 (C3). 240 UECs in total were randomly selected with stratification for further clinical, pathologic and genomic review (C1, $n = 80$; C2, $n = 81$; C3, $n = 79$; see Methods; Fig. 1; Supplementary Fig. S1).

Genomic landscape of endometrioid NSMP-ECs

Overall, in these 240 NSMP-UECs, the most commonly mutated genes were *PTEN* ($n = 154$, 64%), *ARID1A* ($n = 108$, 45%), *PIK3CA* ($n = 102$, 42.5%), *CTNNB1* ($n = 86$, 36%), *PIK3R1* ($n = 77$, 32%), *KRAS* ($n = 70$, 29%), *CTCF* ($n = 34$, 14%) and *BCOR* ($n = 3$, 14%). Other recurrent alterations included *FBXW7*, *SOX17*, *FGFR2* (all $n = 21$, 9%) and *ESR1* ($n = 20$, 8%; Fig. 2A).

Of the 240 NSMP-UECs included in this study, 127 (52.9%) had alterations in combinations of *PTEN*/*PIK3CA* and *PTEN*/*PIK3R1*, other tumors had pathogenic mutations in *AKT1* (6%) and *MTOR* (3%). *KRAS*, *FGFR2* oncogenic mutations and *ERBB2* amplification/activating mutations occurred in a mutually exclusive pattern in 29%, 10%, and 4% of NSMP-UECs, respectively. *CTNNB1* hotspot mutations were present in 36% ($n = 87$) of NSMP-UECs, and there was mutual exclusivity between *KRAS/FGFR2/ERBB2* and *CTNNB1* alterations (DISCOVER $P < 0.001$; Fig. 2B).

As a next step, the genomic landscape of NSMP-UECs according to the clusters was assessed and found to be distinct in terms of their genomic instability, mutational burden, CN and mutational landscapes (Fig. 3). The fraction of genome altered, a measure of chromosomal instability, was significantly higher in the C3 NSMP-UECs compared to NSMP-UECs from the other two clusters (mean 0.17 versus 0.07, ANOVA $P = 0.0002$; Fig. 3B). Overall, amplifications and homozygous deletions were rare in the NSMP-UECs, with *ERBB2* ($n = 5$), *AKT3* ($n = 4$), and *NTRK1* ($n = 4$) amplification and *CDKN2A* deletions ($n = 4$) being the most common. In terms of broad chromosomal arm level alterations, 1q gains were common in C3 ($n = 35$, 44.9%) and C1 tumors ($n = 24$, 30.4%), and less common in C2 tumors ($n = 14$, 17.5%, X^2 $P = 0.001$; Figs. 2A, 3A).

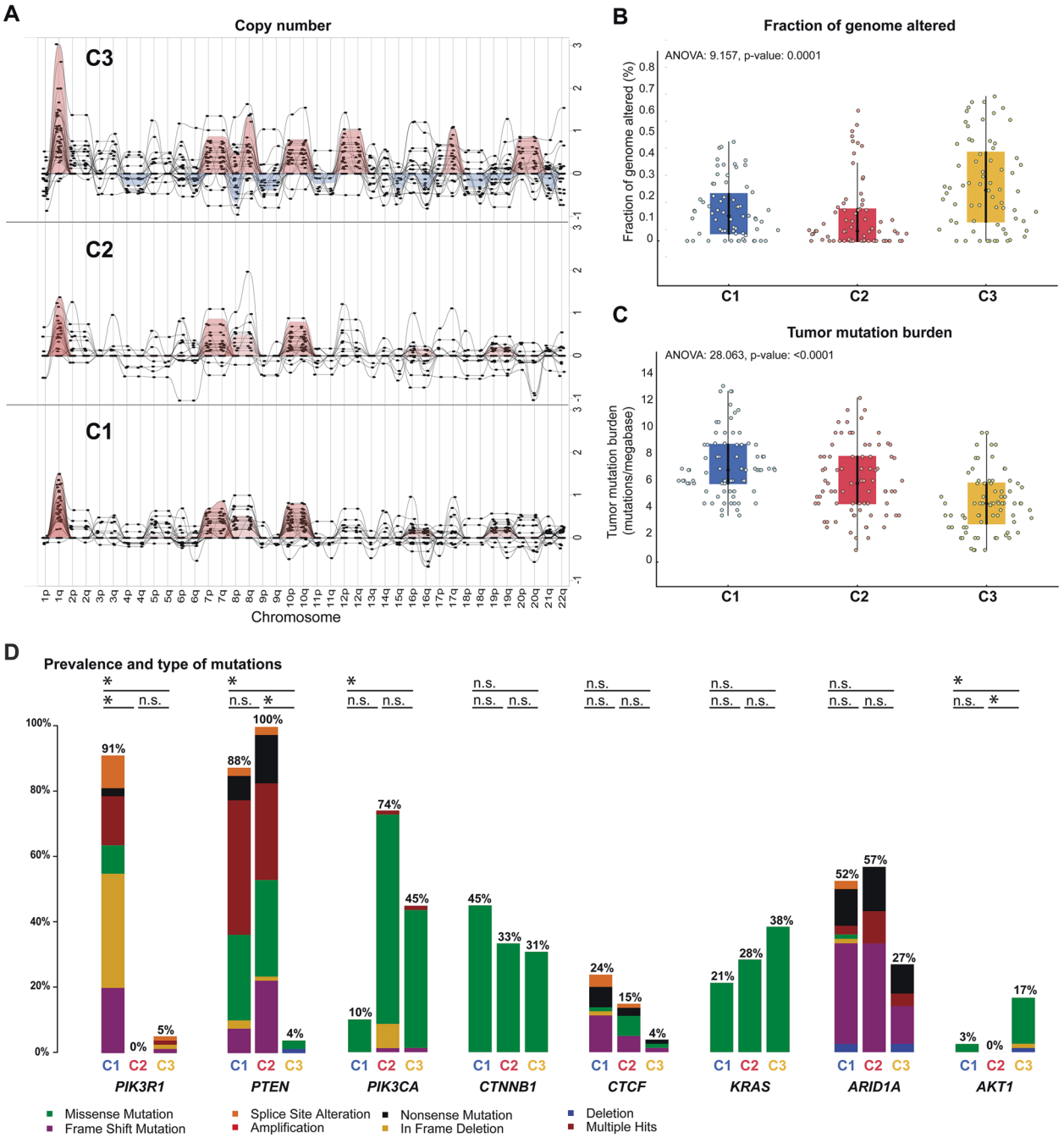

Fig. 3 Global genomic landscape of NSMP uterine endometrioid carcinomas. A Summary of broad copy number alterations in the three molecular clusters of uterine endometrioid carcinomas of no special molecular profile (NSMP-UEC) based on GISTIC results. Each column indicates a chromosomal arm as shown in the X-axis labels. The Y-axis represents G-score which considers the amplitude of the aberration as well as the frequency of its occurrence across samples. **B** Comparison of fraction of genome altered values across the three NSMP-EC clusters. **C** Comparison of tumor mutational burden (number of mutations/megabase) across the three NSMP-UEC clusters. **D** Bar-plots comparing the alteration frequency of 8 commonly altered genes among the three molecular clusters of NSMP-UEC. The black horizontal lines marked with a * at the top of each bar-plot represent statistically significant difference in the frequency of the altered gene among the clusters; n.s. not significant. C1, Cluster 1; C2, Cluster 2; C3, Cluster 3.

The tumor mutational burden progressively decreased from C1 to C3 NSMP-UECs (median number of somatic mutations per megabase for C1, C2 and C3: 6.9, 5.9, 4.4, respectively ANOVA *P*: 0.0001; Table 1, Fig. 3C). When assessing specific mutations, we found that while *PTEN* alterations were common in the C1 and C2 clusters (88 and 100% respectively), they were rare in C3 NSMP-UECs (5%, X^2 $P < 0.0001$; Fig. 3D). *PIK3R1* mutations, which were primarily truncating, were almost exclusively found in C1 tumors (91%; versus 0% in C2 and 5% in C3, X^2 $P < 0.0001$). Conversely, *PIK3CA* mutations, which preferentially affected the hotspot kinase domain codon H1047 (21.4%) or the helical domain hotspot codons E545 and E542 (10.7%, 4.5%), were uncommon in C1 (10%), but had higher frequencies in C2 and C3 NSMP-UECs (74 and 45%, X^2 $P < 0.0001$). *AKT1* mutations, primarily the E17K

Table 1. Summary of genomic findings in the three clusters of uterine endometrioid carcinomas of no special molecular profile (NSMP-UEC).

		Cluster 1 ($n = 80$)	Cluster 2 ($n = 81$)	Cluster 3 ($n = 79$)	All cases ($n = 240$)	*P* value
Tumor mutation burden (mutations/ megabase)	Median	7.00	5.9	4.4	6.00	<0.0001
	95% IQR	6–10	4.4–7.9	2.9–5.9	2–12	
Fraction of genome altered (%)	Median	0.05	0.00	0.09	0.04	<0.0001
	95% IQR	0–0.12	0–0.06	0–0.62	0.02–0.22	
DNA ploidy	Median	2.16	2.03	2.19	2.14	0.498
	95% IQR	2.00–2.35	2.00–2.33	2.00–2.48	2.00–2.41	
Chromosome 1q total copy number	Median	2.2	2.00	2.60	2.00	<0.0001
	95% IQR	2–2.61	1.92–2	2–3.01	2–2.61	
PTEN alterations	*n* (%)	70 (88%)	81 (100%)	3 (4%)	154 (64%)	<0.0001
PIK3R1 alterations	*n* (%)	73 (91%)	0 (0%)	4 (5%)	77 (32%)	<0.0001
PIK3CA alterations	*n* (%)	8 (10%)	60 (74%)	35 (45%)	102 (42%)	<0.0001
AKT1 alterations	*n* (%)	2 (3%)	0 (0%)	13 (17%)	15 (6%)	<0.0001
KRAS alterations	*n* (%)	18 (21%)	22 (28%)	30 (38%)	70 (29%)	0.106
CTNNB1 alterations	*n* (%)	35 (45%)	28 (33%)	23 (31%)	86 (36%)	0.0979
ARID1A alterations	*n* (%)	41 (52%)	45 (57%)	22 (27%)	108 (45%)	0.0004

IQR Interquartile range, *n* Number.

hotspot mutation, were almost exclusively found in C3 NSMP-UECs (17% versus 3% in C1 and 0% in C2, X^2 $P < 0.0001$; Fig. 3D), and they frequently co-occurred with *CTNNB1* mutations (see below). No statistically significant difference in the frequency of alterations affecting *CTNNB1*, *KRAS* and *CTCF* was found between the clusters (X^2 $P > 0.05$ for all). We noted that the majority of non-synonymous somatic mutations identified in NSMP-UECs were oncogenic or likely/predicted oncogenic (72.9%; Supplementary Figs S2 and S3), including *ESR1* mutations involving codons L536, Y537 and D538 which are associated with resistance to hormone therapy in breast cancer[25].

Finally, we evaluated the cancer cell fractions/clonality of the mutations identified, meaning the bioinformatically inferred percentage of cancer cells harboring a given mutation in a tumor sample. This analysis revealed that in C1 NSMP-UECs *PTEN* mutations had the highest cancer cell fractions, and were primarily clonal, whereas *PIK3R1*, *ARID1A* and *KRAS* mutations occurred at lower cancer cell fractions. The same trend was observed in C2 NSMP-UECs with *PTEN* mutations having the highest cancer cell fractions, and *PIK3CA, ARID1A* and *KRAS* mutations with lower cancer cell fractions. In C3 NSMP-UECs, however, more heterogeneity was observed, with either *AKT1*, *ARID1A* or *KRAS* being clonal events in these tumors (Fig. 4).

Taken together, NSMP-UECs are heterogeneous at the genetic level with C1 tumors being defined by recurrent *PIK3R1* and *PTEN* alterations, C2 tumors by a combination of *PTEN* and *PIK3CA* mutations and C3 tumors by *KRAS* mutations along with 1q high level gain in the absence of *PTEN* alterations or alternatively *AKT1* mutations along with *CTNNB1* mutations.

Evaluation of the interaction matrix between the commonly altered genes in NSMP-UECs showed strong mutual exclusivity between *PIK3CA* and *PIK3R1* mutations (DISCOVER $P < 0.0001$), confirming previous reports[1,13]. In addition, *CTNNB1* and *KRAS* as well as *PTEN* and *AKT1* mutations were also found to be mutually exclusive (DISCOVER $P < 0.01$; Supplementary Fig. S4).

In terms of mutational signatures, 202 cases had sufficient mutations (≥5 mutations) to allow for investigation of mutational signatures. Consistent with previous results[26], signature 1 associated with aging was the most common mutational signature in NSMP-UECs; no statistically significant difference was observed between the 3 clusters (Supplementary Fig. S5).

Genomic landscape of NSMPs of non-endometrioid and variant endometrioid histology

In addition to the 240 NSMPs of endometrioid subtype, 44 additional ECs subjected to clinical sequencing that fulfilled the criteria of NSMP were of non-endometrioid ($n = 19$) or variant ($n = 21$) histologic types. The majority of these non-endometrioid or variant endometrioid NSMP-ECs clustered with C3 UECs (72.7%, $n = 32$); 15.9% clustered with C2 tumors ($n = 7$) and 11.4% clustered with C1 UECs ($n = 5$). One of the two cases of corded and hyalinized endometrioid carcinomas clustered with C2 tumors and the other with C3 tumors.

In terms of global genomic profile, these 44 non-UEC or variant UEC NSMP tumors showed a significantly higher fraction of genome altered (median: 0.0993, range: 0.024–0.76) compared to NSMP-UEC (median: 0.035, range: 0–0.67; Mann-Whitney U $P < 0.0001$; Fig. 4B). Furthermore, non-UEC or variant UEC NSMP tumors had a higher number of intrachromosomal breakpoints (median: 28, range: 23–74) compared to UEC tumors (median: 24, range: 21–72; Mann–Whitney U $P < 0.0001$; data not shown) and had a lower overall number of somatic mutations (median: 5 versus 6 respectively; Mann–Whitney U $P = 0.009$).

The 15 high-grade ECs with ambiguous morphology harbored alterations in *PIK3CA* ($n = 6$), *ARID1A* and *KRAS* ($n = 5$). The clear cell carcinomas had *ARID1A* ($n = 4$) and *PTEN* alterations ($n = 1$; Fig. 4B). The seven mesonephric/mesonephric-like carcinomas all had activating *KRAS* mutations and chromosome 1q gain, with only two cases harboring concurrent *PTEN* or *PIK3CA* mutations[27]. The carcinosarcomas all had *PIK3CA* mutations ($n = 5$) along with either *PTEN* ($n = 3$) or *FBXW7* ($n = 2$) alterations. Both undifferentiated ECs showed truncating mutations in *SMARCA4*. Both variant UEC NSMPs of corded and hyalinized endometrioid carcinoma harbored *MED12* mutations, with one also harboring *PTEN* and *PIK3CA* mutations and the other case a *CTNNB1* mutation. Despite having a variant morphologic phenotype, the molecular phenotype of these tumors closely resembled that of other UECs; however, the limited number of cases prevents any firm conclusion to be drawn (Fig. 4B).

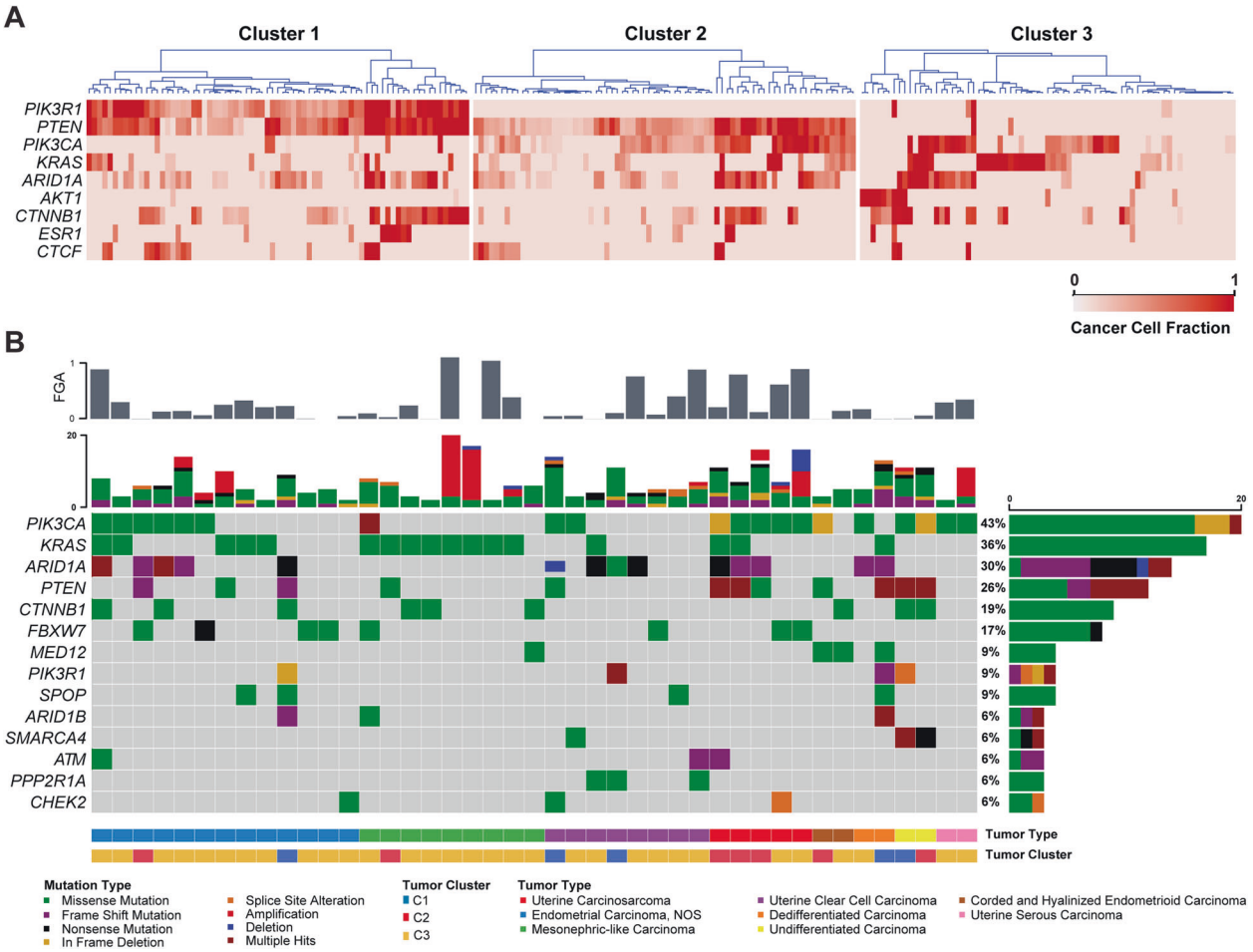

Fig. 4 Clonality of somatic mutations in NSMP uterine endometrioid carcinomas and recurrent genomic alterations in non-endometrioid endometrial cancers of NSMP. A Heatmaps showing the cancer cell fractions of the most commonly altered genes among the three clusters of uterine endometrioid carcinomas of no special molecular profile (NSMP-UEC). Each column represents a tumor. The gradient of the heatmap is based on the calculated cancer cell fraction of the alteration in the sample, color-coded according to the legend. **B** Oncoprint depicting the most recurrent genomic alterations in non-endometrioid endometrial carcinomas of no special molecular profile (NSMP). Each column represents a tumor with the bar graph at the top depicting the number/distribution of alterations per sample, and the Oncoprint rows showing alterations for each gene. The bottom part of the graph shows the summary of histopathologic and clinical information for each case. The bar graph on the right of the panel shows the number and distribution of alterations for each gene. Mutation types and clinicopathologic features are color-coded according to the legend. C1, Cluster 1; C2, Cluster 2; C3, Cluster 3.

Clinicopathologic features of NSMP ECs

Among the NSMP-UEC patients for whom in-depth clinicopathologic review was performed ($n = 240$), the median age at diagnosis was 63 years (range: 28–91 years); there was no statistically significant difference between the clusters in terms of age distribution (Fig. 5A). As expected, age had a strong association with the background endometrium with patients with background atrophic/inactive endometrium being older (median age: 65.5 years) compared to patients with either background endometrial hyperplasia (median age: 59 years) or proliferative endometrium (median age: 50.5 years; ANOVA $P = 0.0001$). Of note, background endometrial hyperplasia was more likely to be observed in C2 ($n = 42$) compared to C1 ($n = 29$) and C3 ($n = 17$) patients (X^2 $P = 0.02$; Fig. 5B), which is in line with prior work showing frequent alteration of *PTEN* and *PIK3CA* in endometrial hyperplasia[28,29] while *PIK3R1* alterations are reportedly rare in hyperplasia[30].

Most of the NSMP-UEC in the cohort were FIGO grade 1 tumors ($n = 117$, 48.7%), followed by FIGO grade 2 ($n = 76$, 31.7%) and FIGO grade 3 tumors ($n = 47$, 19.6%). C3 tumors were more likely to have a high FIGO grade with 30% (24/79) having FIGO grade 3 morphology compared to 14.4% in the other clusters (23/161; X^2 *P*: 0.0001; Fig. 5C).

Estrogen receptor (ER) expression results by immunohistochemical analysis were available for 48 samples; C3 tumors were more likely to have negative or weak and focal ER expression (12/22, 54.5%) compared to C1/C2 tumors (23.1% (6/26); X^2 *P*: 0.025; Supplementary Fig. S6). Progesterone receptor (PR) expression as assessed by immunohistochemistry were available for 33 samples; C3 tumors were more likely to have negative or weak and focal PR expression (9/15, 60%) compared to C1/C2 tumors (16.7% (3/18); X^2 *P*: 0.03; Supplementary Fig. S7).

Patients with C3 NSMP-UECs were more likely to present with higher clinical stage disease with 36.7% (29/79) presenting at FIGO stages III and IV compared to 19.9% (32/161) for C1 and C2 NSMP-UECs (X^2 *P*: 0.005; Table 2). The same was observed for pathologic T stage where 50.6% (40/79) of patients with C3 tumors presented at pathologic T2 stage or above compared to 23.6% (38/161) of C1/C2 tumors (X^2 *P*: < 0.001; Fig. 5F). Follow-up data showed that patients with C3 tumors had a higher mortality rate (49.4%, 39/79) compared to C1 and C2 patients (17.5%, 14/80 and 22.2%, 18/81, respectively; X^2 *P*: 0.0001). Lymphovascular invasion was identified in 78 tumors (32.5%). The C3 tumors were more likely to have lymphovascular invasion compared to the other clusters (41.8%, 33/79 versus 27.9%, 45/161 for C1/C2, X^2 *P*: 0.032). On the other

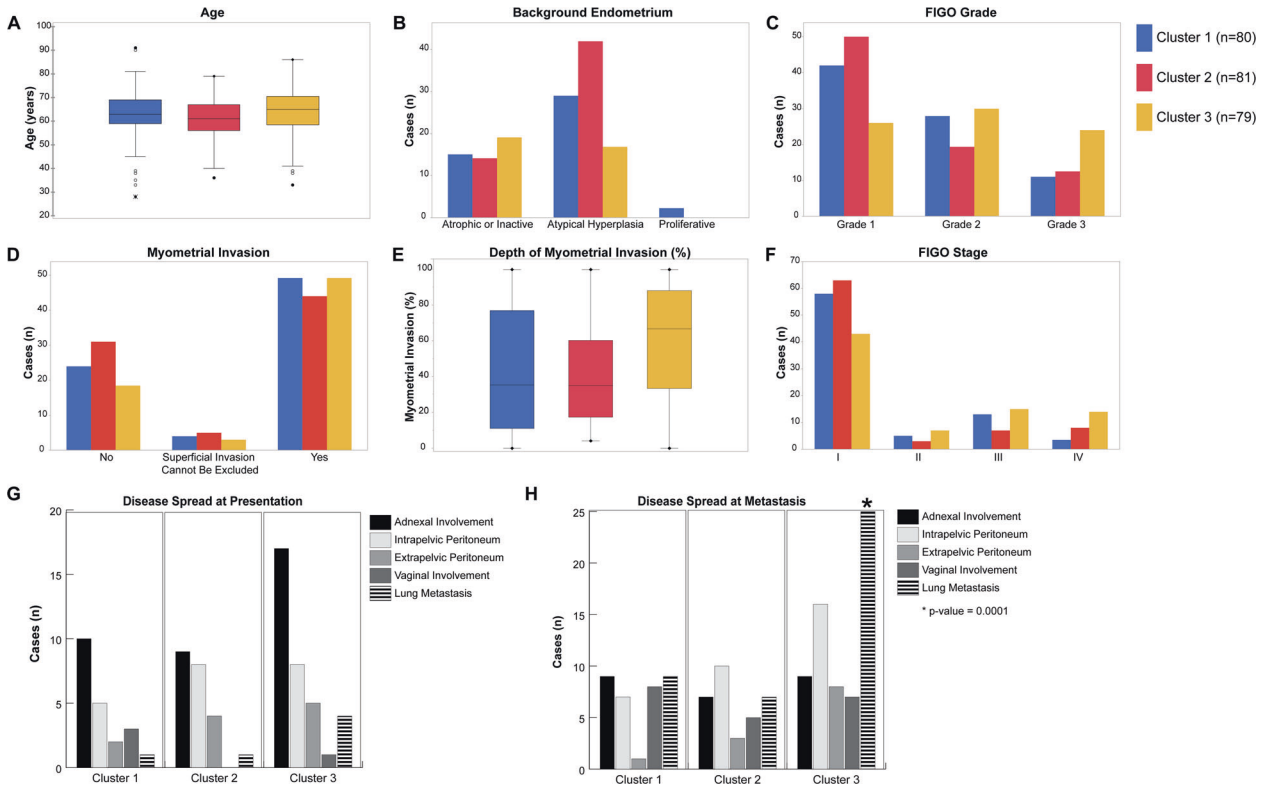

Fig. 5 Clinicopathologic features of NSMP uterine endometrioid carcinomas. A Box and whisker plots comparing age distribution between the molecular clusters of uterine endometrioid carcinomas of no special molecular profile (NSMP-UEC). **B** Bar-plot comparing the background endometrium findings among the molecular clusters. **C** Bar-plot comparing the tumor FIGO grade among the molecular clusters. **D** Bar-plot comparing the distribution of myometrial invasion among the molecular clusters. **E** Box and whisker plots comparing the depth of myometrial invasion among the molecular clusters. **F** Bar-plot comparing the distribution of tumor FIGO clinical stage among the molecular clusters. **G** Bar-plot comparing the tumor spread at the time of diagnosis among molecular clusters. **H** Bar-plot comparing the tumor spread at the time of recurrence among molecular clusters. Molecular clusters are color coded with blue representing Cluster 1, red representing Cluster 2 and yellow representing Cluster 3 tumors.

hand, C1/C2 tumors were more likely to have lymph node metastasis (62.7%, 101/161 versus 39.2%, 31/79; X^2 *P*: 0.001) than C3 tumors (Table 2).

Patients with C3 NSMP-UECs were more likely to have lung metastasis at recurrence (25/79 versus 16/161 for C1 and C2; X^2 *P*: 0.0001), and to have involvement of extra-pelvic peritoneum and omentum on recurrence (16 and 8 out of 79 cases, respectively) compared to C1/C2 tumors (17 and 4 out of 161 cases, respectively; X^2 $P = 0.04$ and 0.011; Fig. 5G, H).

Among genomic factors, 1q high level gain, absence of *PTEN* mutation and presence of *AKT1* mutation were strongly associated with lung metastasis (X^2 $P = 0.0001$, 0.0001 and 0.005 respectively). Tumors with *KRAS* mutations in isolation were not associated with lung metastasis (X^2 $P = 0.167$), however in combination with an absence of *PTEN* mutations the association with lung metastasis was significant. Furthermore, 1q gain was associated with increased likelihood of myometrial invasion (91.3% ($n = 63/69$) vs. 59.6% ($n = 102/171$); X^2 $P = 0.0001$). Among the genomic alterations in our entire cohort, *ESR1* mutations showed a strong correlation with age; patients with *ESR1* mutations were strictly post-menopausal with a median age of 69 years (range 60–82 years) while the patients without *ESR1* mutations were younger and included premenopausal patients (median age 62, range: 28–91 years; Mann–Whitney-U $P = 0.0001$).

From the 284 patients with NSMP-EC, 171 patients were seen at the time of initial treatment planning with surgery performed at MSK, whereas the remainder of the patients ($n = 113$) were seen at the time of recurrence. As an exploratory, hypothesis-generating analysis, we assessed whether the different clusters of NSMP-ECs identified would be associated with outcome (Fig. 6). Mortality and disease recurrence were more likely in patients with C3 tumors with a 45.3% mortality rate (24/53) and a 66% recurrence rate (35/53). In contrast, patients with C1 and C2 tumors had lower mortality rates (5.3% (3/54) and 18.7% (13/64), respectively) and lower recurrence rates (31.9% (17/54) and 25% (16/64), respectively; Fig. 6E). Log-rank survival analysis showed that the molecular clusters were associated with distinct overall survival (OS), with patients with C1 tumors having the best survival outcomes (Log-rank *P*: 0.0005; Fig. 6A), while C2 and C3 tumors were statistically similar. In terms of disease-free survival (DFS), patients with C3 tumors had the worse outcomes, however, C1 and C2 tumors together showed similar DFS curves (Log-rank *P*: < 0.0001; Fig. 6B). Multivariate Cox-regression survival analysis showed that tumor clusters conferred OS disadvantage with C2 tumors having a hazard ratio (HR) of 3.7 and C3 tumors having a hazard ratio of 4.0 (*P*: 0.049 and 0.032 respectively). However, tumor clusters were not associated with disease-free survival on multivariate analysis. Interestingly, after controlling for stage, the most important prognostic factors for both OS and DFS were presence of FIGO grade 3 morphology (OS HR: 19.6 (*P*: 0.0003), DFS HR: 10.5 ($P < 0.0001$)) and non-endometrioid morphology (OS HR: 30.6, $P < 0.0001$; DFS HR: 12.9, $P < 0.0001$; Fig. 6C, D; Supplementary Table S1).

DISCUSSION

The NSMP-EC have been shown to have considerable morphologic and clinical diversity: In comparison with copy number-high or

Table 2. Summary of clinicopathologic findings in the three clusters of uterine endometrioid carcinomas of no special molecular profile (NSMP-UEC).

	Cluster 1 (*n*, %)	Cluster 2 (*n*, %)	Cluster 3 (*n*, %)	All Cases (*n*, %)
Age median (*n*, min/max)	63 (28–91)	61 (36–79)	65 (33–86)	63 (28–91)
Tumor FIGO stage				
I	58 (72.5%)	63 (77.8%)	43 (54.4%)	164 (68.3%)
II	5 (6.2%)	3 (3.7%)	7 (8.9%)	15 (6.25%)
III	13 (16.2%)	7 (8.6%)	15 (19%)	35 (14.6%)
IV	4 (5%)	8 (9.9%)	14 (17.7%)	26 (10.8%)
Disease status				
Disease free	42 (52.5%)	51 (63%)	18 (22.8%)	111 (46.3%)
Persisted/ recurred/ progressed	38 (47.5%)	30 (37%)	61 (77.2%)	129 (53.7%)
Survival status				
Alive	66 (82.5%)	63 (77.8%)	40 (50.6%)	169 (70.4%)
Deceased	14 (17.5%)	18 (22.2%)	39 (49.4%)	71 (29.6%)
Tumor FIGO grade				
Grade I–II	69 (86.2%)	69 (85.2%)	55 (69.6%)	193 (80.4%)
Grade III	11 (13.7%)	12 (14.8%)	24 (30.4%)	47 (19.6%)
Tumor myometrial invasion				
Absent	24 (30%)	31 (38.3%)	18 (22.8%)	73 (30.4%)
Superficial invasion cannot be excluded	4 (5%)	5 (6.2%)	3 (3.8%)	12 (5%)
Present	49 (61.2%)	44 (54.3%)	49 (62%)	142 (59.2%)
N/A	3 (3.7%)	1 (1.2%)	9 (11.4%)	13 (5.4%)
Cervical stromal invasion				
Absent	67 (83.7%)	69 (85.2%)	51 (64.6%)	187 (77.9%)
Present	10 (12.5%)	9 (11.1%)	19 (24%)	38 (15.8%)
N/A	3 (3.7%)	3 (3.7%)	9 (11.4%)	15 (6.2%)
Lymphovascular invasion				
Absent	52 (65%)	58 (71.6%)	36 (45.5%)	146 (60.8%)
Present	23 (28.7%)	22 (27.2%)	33 (41.8%)	78 (32.5%)
N/A	5 (6.2%)	1 (1.2%)	10 (12.7%)	16 (6.7%)

N/A not available/missing data.

POLE ECs, patients with NSMP-EC have an intermediate prognosis comparable to that of women with MSI-H ECs[1]. However, considerable heterogeneity within the NSMP category exists in terms of clinical outcomes as some patients have an excellent prognosis, whereas others have a more aggressive disease course with associated morbidity and mortality[3,6]. While the majority of NSMP-EC are endometrioid, other morphologic variants including those with ambiguous morphology, endometrial clear cell carcinoma, mesonephric-like carcinoma, and other rare morphologic variants have been previously reported[31]. Current management of NSMP-EC is mainly driven by clinical stage and histopathologic features such as FIGO grade, and presence of lymphovascular invasion[32]. Recently, molecular features such as *CTNNB1* alterations or L1CAM expression have been used in risk stratification of the NSMP tumors[33].

Our results demonstrate that the clinical and pathologic heterogeneity of the NSMP-ECs can be largely explained with the underlying molecular alterations. In fact, our results suggest that NSMP-ECs, which comprise the largest share of EC molecular subtypes, are composed of several distinct molecular subclades; based on clustering of mutations in cancer-related genes and copy number alterations, we have shown that NSMP-ECs are composed of at least 3 distinct molecular clusters: The first two clusters appear to be to be driven by activating alterations of the PI3K pathway, where mutations in *PTEN* are often paired with truncating alterations of *PIK3R1* (C1) or with activating *PIK3CA* mutations (C2). Analysis of cancer cell fractions suggests that *PTEN* alterations are the initiating event for C1 and C2 tumors followed by alterations in either *PIK3CA* or *PIK3R1*, *ARID1A*, *CTNNB1* and *KRAS*.

C3 tumors are markedly different from both C1 and C2 tumors. These tumors have a relative dearth of *PTEN* alterations. PI3K pathway alterations in C3 tumors were mostly single hits with either *PIK3CA* or *AKT1* or *KRAS* activating alterations. A subset of C3 tumors harbored *KRAS* activating mutations along with chromosome 1q high level gain. The latter finding has been well-studied and believed to be associated with a mesonephric-like phenotype[34] with often adverse outcomes[35]. The mesonephric-like carcinomas are known to have a propensity for lung metastasis[36], a phenomenon which we also observed in our cohort. Unlike the *KRAS* mutated/1q gain tumors, which are well documented, characterization of an *AKT1* mutated subgroup has only been observed anecdotally[37]. In this study, we report an even stronger propensity for lung metastasis compared to the *KRAS* mutated/1q gain tumors.

The genomic landscape of C1 and C2 NSMP-ECs supports the previous findings of the synergistic effect of *PTEN* and *PIK3CA* mutations[38–40], and in the absence of *PIK3CA* activating mutations, *PIK3R1* truncating mutations may exert a similar synergistic effect[38,40,41]. The mutually exclusive nature of *PIK3R1* and *PIK3CA* mutations has been previously shown in both endometrial and

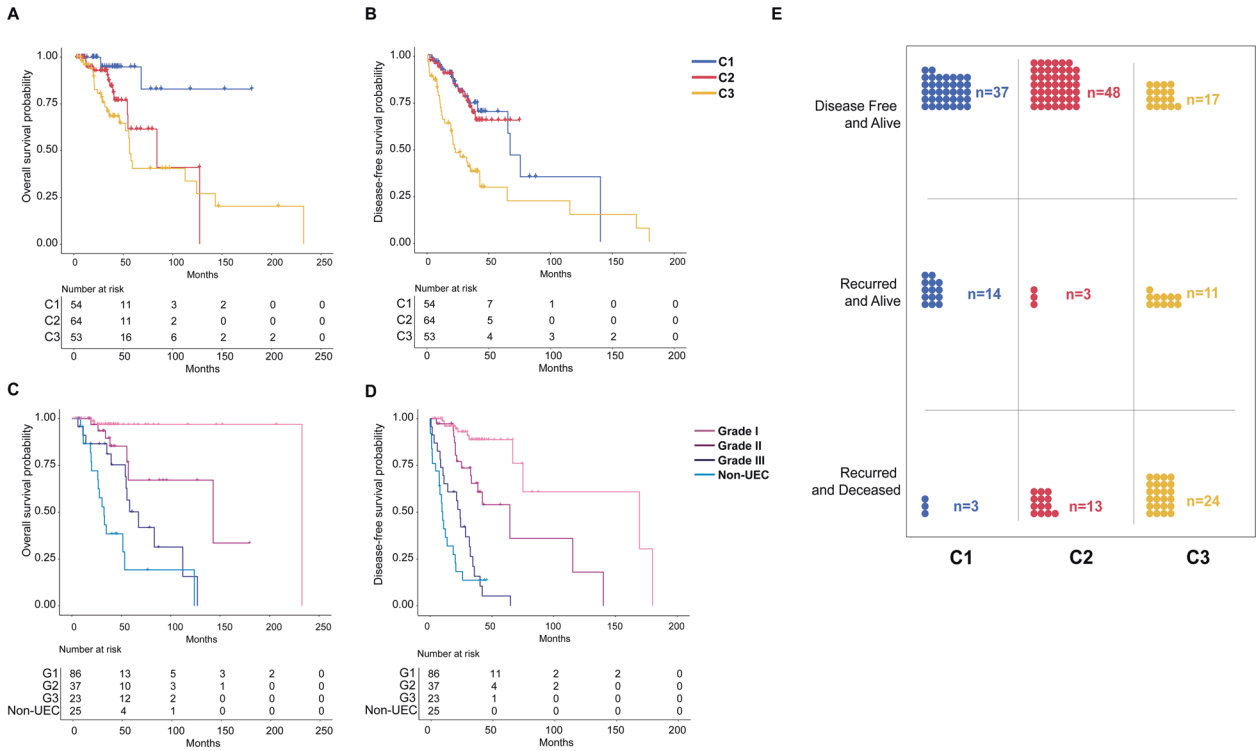

Fig. 6 Association of molecular clusters and histologic grade with outcome in NSMP uterine endometrial carcinomas. A, **B** Kaplan–Meier curves comparing overall survival and disease-free survival among molecular clusters of NSMP-EC. **C**, **D** Kaplan–Meier curves comparing overall survival and disease-free survival among histologic grades and type of NSMP-EC. **E** Distribution of outcome events among the three molecular clusters of NSMP-EC. C1, Cluster 1; C2, Cluster 2; C3, Cluster 3; G1-G3, Grades 1 through 3.

breast cancers[1,42]. *AKT1* p.E17K mutation is another activating mechanism of the PI3K/AKT pathway[43,44] and we have shown that activating mutations of *AKT1* gene occur in absence of alterations of upstream *PTEN/PIK3CA/PIK3R1*, thereby defining a novel molecular subcategory of NSMP-ECs.

Of interest *CTNNB1* gene alterations were observed in relatively equal proportions in all three clusters (27–49% of samples). While other reports suggest adverse clinical outcomes associated with *CTNNB1* alterations[45–47], in our cohort, *CTNNB1* hotspot mutations did not show any adverse survival effect. However, the previous studies did not follow the ProMisE classification and were limited to UECs, which may explain the different results observed in our cohort[45–47].

The molecular clustering of the NSMP-EC may portend clinical and prognostic significance. In our cohort, multivariate analysis showed a statistically significant OS hazard ratio associated with C2 and C3 tumors. Our findings suggest that NSMP-EC should be considered as separate molecular clades rather than a single group of clinically, pathologically, and molecularly heterogenous tumors. Previously, it was suggested that clustering of NSMP-EC based on 1q high level gain can also successfully separate the tumors into prognostic groups[6,9], however, in our cohort, 1q copy number status alone was not prognostically significant in multivariate analysis (see Supplementary Table S1).

In conclusion, we have shown here that the NSMP-EC molecular subset of endometrial carcinomas can be further subclassified based on their molecular landscape and that these molecular clusters are associated with meaningful clinical differences. We suggest that cluster 1 and 2 NSMP-EC can perhaps be defined as a *PTEN* and PI3K altered NSMP-EC group, and the cluster 3 tumors designated as either 1) *PTEN* wild-type *AKT1* altered NSMP-EC or 2) *PTEN* wild-type *KRAS* altered NSMP-EC or 3) *PTEN* wild-type *PIK3CA* altered NSMP-EC. Further evaluation is needed to confirm the clinical or prognostic significance of these clusters.

DATA AVAILABILITY

The datasets used and analyzed in the current study are available from the corresponding authors upon reasonable request.

REFERENCES

1. Cancer Genome Atlas Network. Integrated genomic characterization of endometrial carcinoma. *Nature* **497**, 67–73 (2013).
2. McAlpine, J., Leon-Castillo, A. & Bosse, T. The rise of a novel classification system for endometrial carcinoma; integration of molecular subclasses. *J. Pathol.* **244**, 538–549 (2018).
3. Talhouk, A. et al. Confirmation of ProMisE: a simple, genomics-based clinical classifier for endometrial cancer. *Cancer* **123**, 802–813 (2017).
4. Murali, R. et al. High-grade endometrial carcinomas: morphologic and immunohistochemical features, diagnostic challenges and recommendations. *Int. J. Gynecol. Pathol.* **38**, S40–S63 (2019).
5. Bosse, T. et al. Molecular classification of grade 3 endometrioid endometrial cancers identifies distinct prognostic subgroups. *Am. J. Surg. Pathol.* **42**, 561–568 (2018).
6. Depreeuw, J. et al. Amplification of 1q32.1 refines the molecular classification of endometrial carcinoma. *Clin. Cancer Res.* **23**, 7232–7241 (2017).
7. Stelloo, E. et al. Improved risk assessment by integrating molecular and clinicopathological factors in early-stage endometrial cancer-combined analysis of the portec cohorts. *Clin. Cancer Res.* **22**, 4215–4224 (2016).
8. Kommoss, F. K. et al. L1CAM further stratifies endometrial carcinoma patients with no specific molecular risk profile. *Br. J. Cancer* **119**, 480–486 (2018).
9. Vermij, L., Smit, V., Nout, R. & Bosse, T. Incorporation of molecular characteristics into endometrial cancer management. *Histopathology* **76**, 52–63 (2020).
10. Zehir, A. et al. Mutational landscape of metastatic cancer revealed from prospective clinical sequencing of 10,000 patients. *Nat. Med.* **23**, 703 (2017).
11. Cheng, D. T. et al. Memorial sloan kettering-integrated mutation profiling of actionable cancer targets (MSK-IMPACT): a hybridization capture-based next-generation sequencing clinical assay for solid tumor molecular oncology. *J. Mol. Diagn.* **17**, 251–264 (2015).
12. Talhouk, A. et al. A clinically applicable molecular-based classification for endometrial cancers. *Br. J. Cancer* **113**, 299–310 (2015).

13. Momeni-Boroujeni, A. et al. Clinicopathologic and genomic analysis of TP53-mutated endometrial carcinomas. *Clin. Cancer Res.* **27**, 2613–2623 (2021).
14. Middha, S. et al. Reliable pan-cancer microsatellite instability assessment by using targeted next-generation sequencing data. *JCO Precis. Oncol.* **1**, 1–17 (2017).
15. Mermel, C. H. et al. GISTIC2.0 facilitates sensitive and confident localization of the targets of focal somatic copy-number alteration in human cancers. *Genome Biol* **12**, R41 (2011).
16. Shen, R. & Seshan, V. E. FACETS: allele-specific copy number and clonal heterogeneity analysis tool for high-throughput DNA sequencing. *Nucleic Acids Res.* **44**, e131 (2016).
17. Carter, S. L. et al. Absolute quantification of somatic DNA alterations in human cancer. *Nat. Biotechnol.* **30**, 413–421 (2012).
18. Diaz-Gay, M. et al. Mutational signatures in cancer (MuSiCa): a web application to implement mutational signatures analysis in cancer samples. *BMC Bioinform.* **19**, 224 (2018).
19. Chakravarty, D. et al. OncoKB: a precision oncology knowledge base. *JCO Precis. Oncol.* **2017**, 1–16 (2017).
20. Canisius, S., Martens, J. W. & Wessels, L. F. A novel independence test for somatic alterations in cancer shows that biology drives mutual exclusivity but chance explains most co-occurrence. *Genome Biol.* **17**, 1–17 (2016).
21. Carlson, J. & McCluggage, W. G. Reclassifying endometrial carcinomas with a combined morphological and molecular approach. *Curr. Opin. Oncol.* **31**, 411–419 (2019).
22. Hoang, L. N. et al. Interobserver agreement in endometrial carcinoma histotype diagnosis varies depending on the cancer genome atlas (TCGA)-based molecular subgroup. *Am. J. Surg. Pathol.* **41**, 245–252 (2017).
23. Van Der Maaten, L. Accelerating t-SNE using tree-based algorithms. *J. Mach. Learn. Res.* **15**, 3221–3245 (2014).
24. Hahsler, M., Piekenbrock, M. & Doran, D. dbscan: fast density-based clustering with R. *J. Stat. Softw.* **91**, 1–30 (2019).
25. Szostakowska, M., Trebinska-Stryjewska, A., Grzybowska, E. A. & Fabisiewicz, A. Resistance to endocrine therapy in breast cancer: molecular mechanisms and future goals. *Breast Cancer Res. Treat.* **173**, 489–497 (2019).
26. Ashley, C. W. et al. Analysis of mutational signatures in primary and metastatic endometrial cancer reveals distinct patterns of DNA repair defects and shifts during tumor progression. *Gynecol. Oncol.* **152**, 11–19 (2019).
27. da Silva, E. M. et al. Mesonephric and mesonephric-like carcinomas of the female genital tract: molecular characterization including cases with mixed histology and matched metastases. *Mod. Pathol.* **34**, 1570–1587 (2021).
28. Hayes, M. P. et al. PIK3CA and PTEN mutations in uterine endometrioid carcinoma and complex atypical hyperplasia. *Clin. Cancer Res.* **12**, 5932–5935 (2006).
29. Hsu, A. H. et al. Crosstalk between PKCα and PI3K/AKT signaling is tumor suppressive in the endometrium. *Cell Rep.* **24**, 655–669 (2018).
30. Russo, M. et al. Mutational profile of endometrial hyperplasia and risk of progression to endometrioid adenocarcinoma. *Cancer* **126**, 2775–2783 (2020).
31. Stelloo, E. et al. Refining prognosis and identifying targetable pathways for high-risk endometrial cancer; a TransPORTEC initiative. *Mod. Pathol.* **28**, 836–844 (2015).
32. Koh, W. J. et al. Uterine Neoplasms, Version 1.2018, NCCN Clinical Practice Guidelines in Oncology. *J. Natl Compr. Cancer Netw.* **16**, 170–199 (2018).
33. Urick, M. E. & Bell, D. W. Clinical actionability of molecular targets in endometrial cancer. *Nat. Rev. Cancer* **19**, 510–521 (2019).
34. Na, K. & Kim, H. S. Clinicopathologic and molecular characteristics of mesonephric adenocarcinoma arising from the uterine body. *Am. J. Surg. Pathol.* **43**, 12–25 (2019).
35. Euscher, E. D. et al. Mesonephric-like carcinoma of the endometrium: a subset of endometrial carcinoma with an aggressive behavior. *Am. J. Surg. Pathol.* **44**, 429–443 (2020).
36. Pors, J. et al. Clinicopathologic characteristics of mesonephric adenocarcinomas and mesonephric-like adenocarcinomas in the gynecologic tract: a multi-institutional study. *Am. J. Surg. Pathol.* **45**, 498–506 (2021).
37. Shoji, K. et al. The oncogenic mutation in the pleckstrin homology domain of AKT1 in endometrial carcinomas. *Br. J. Cancer* **101**, 145–148 (2009).
38. Wang, Y. et al. Genomic comparison of endometrioid endometrial carcinoma and its precancerous lesions in chinese patients by high-depth next generation sequencing. *Front. Oncol.* **9**, 123 (2019).
39. Nout, R. A. et al. Improved risk assessment of endometrial cancer by combined analysis of MSI, PI3K-AKT, Wnt/beta-catenin and P53 pathway activation. *Gynecol. Oncol.* **126**, 466–473 (2012).
40. Cheung, L. W. et al. High frequency of PIK3R1 and PIK3R2 mutations in endometrial cancer elucidates a novel mechanism for regulation of PTEN protein stability. *Cancer Discov.* **1**, 170–185 (2011).
41. Thorpe, L. M. et al. PI3K-p110alpha mediates the oncogenic activity induced by loss of the novel tumor suppressor PI3K-p85alpha. *Proc. Natl Acad. Sci. USA* **114**, 7095–7100 (2017).
42. Chen, L. et al. Characterization of PIK3CA and PIK3R1 somatic mutations in Chinese breast cancer patients. *Nat. Commun.* **9**, 1357 (2018).
43. Cohen, Y. et al. AKT1 pleckstrin homology domain E17K activating mutation in endometrial carcinoma. *Gynecol. Oncol.* **116**, 88–91 (2010).
44. Wu, W. et al. Effects of AKT1 E17K mutation hotspots on the biological behavior of breast cancer cells. *Int. J. Clin. Exp. Pathol.* **13**, 332–346 (2020).
45. Kurnit, K. C. et al. CTNNB1 (beta-catenin) mutation identifies low grade, early stage endometrial cancer patients at increased risk of recurrence. *Mod. Pathol.* **30**, 1032–1041 (2017).
46. Costigan, D. C., Dong, F., Nucci, M. R. & Howitt, B. E. Clinicopathologic and Immunohistochemical Correlates of CTNNB1 Mutated Endometrial Endometrioid Carcinoma. *Int. J. Gynecol. Pathol.* **39**, 119–127 (2020).
47. Liu, Y. et al. Clinical significance of CTNNB1 mutation and Wnt pathway activation in endometrioid endometrial carcinoma. *J. Natl Cancer Inst.* **106**, dju245 (2014).

AUTHOR CONTRIBUTIONS

R.A. Soslow and A. Momeni-Boroujeni conceived the study. B. Nguyen and C.M. Vanderbilt performed bioinformatics analyses. A. Momeni-Boroujeni, B. Nguyen, C. M. Vanderbilt, M. Ladanyi, N.R. Abu-Rustum, C. Aghajanian, L.H. Ellenson, B. Weigelt, R.A. Soslow interpreted results. A. Momeni-Boroujeni, R.A. Soslow and B. Weigelt drafted the manuscript. All authors reviewed and approved the final version of the manuscript.

FUNDING

BW was funded in part by Breast Cancer Research Foundation and Cycle for Survival grants. Research reported in this publication was supported in part by a Cancer Center Support Grant of the NIH/NCI (Grant No. P30CA008748).

ETHICS APPROVAL AND CONSENT TO PARTICIPATE

This study was approved by the Memorial Sloan Kettering Cancer Center Institutional Review Board and written informed consent was obtained from all patients.

COMPETING INTERESTS

C.A. reports membership of advisory boards/ personal fees from Tesaro, Eisai/Merck, Mersana Therapeutics, Roche/Genentech, Abbvie, AstraZeneca/Merck, Repare Therapeutics, and grants from Clovis, Genentech, AbbVie, Astra Zeneca, all outside the submitted work. N.R. Abu-Rustum reports Stryker/ Novadaq and GRAIL grants paid to the institution, outside the current study. B.W. reports ad hoc membership of the scientific advisory board of REPARE Therapeutics, outside the submitted work. The remaining authors have no competing interests to disclose.

ADDITIONAL INFORMATION

Supplementary information The online version contains supplementary material available at https://doi.org/10.1038/s41379-022-01066-y.

Correspondence and requests for materials should be addressed to Britta Weigelt or Robert A. Soslow.